Int J Clin Exp Med 2019;12(5):4781-4793
www.ijcem.com /ISSN:1940-5901/IJCEM0019057

Original Article

N-substituted 2-(2-oxo-2H-chromen-4-yloxy) propanamide: synthesis and inhibition of acute renal injury by controlling TGF-β1

Lei Liu[1*], Dong Wang[2*], Yi-Ming Zhang[2], Ming-Ming Wei[2], Xue Meng[2], Kun Zhang[2], Nan Zhang[2], Shao-Qing Zhang[2], Xin-Jian Li[2]

[1]*Department of General Practice, Affiliated Hospital of Jining Medical College, Jining 272000, Shangdong, China;* [2]*Department of Nephrology, Affiliated Hospital of Jining Medical College, Jining 272000, Shangdong, China.* [*]*Equal contributors.*

Received November 3, 2015; Accepted February 10, 2016; Epub May 15, 2019; Published May 30, 2019

Abstract: A new series of N-substituted 2-(2-oxo-2H-chromen-4-yloxy)propanamide derivatives were synthesized by converting 4-hydroxy coumarin to the corresponding ethyl 2-(2-oxo-2Hchromen-4-yloxy)propanoate followed by hydrolysis and coupling with different amines. All the compounds were tested against renal cell apoptosis. Compound 7 markedly reduced the injury-induced tubular lesions, renal cell apoptosis, and normalized the injury induced renal dysfunction. Compound 7 treatment inhibited the injury-induced elevation of inflammatory factors and Tgf-β1, as well as apoptosis. The present study therefore suggests C7 may be a therapeutic candidate for treating acute kidney injury.

Keywords: N-substituted 2-(2-oxo-2H-chromen-4-yloxy)propanamide, acute renal injury, TGF-β1

Introduction

Renal ischemia/reperfusion (I/R) injury will commonly occur after major surgery or renal transplantation in both allograft and native kidneys, which is the most common cause of acute kidney injury (AKI) [1]. AKI is having more than 5% of effect of all hospitalized patients with an unacceptably high rate of mortality [2].

There is no effective therapy currently available for AKI [3]. Renal I/R injury causes primary tubular epithelial cell injury, together with tubular obstruction and reduced tubular re-absorption of NaCl. But, a number of studies reported that hemodynamic changes induced by renal I/R injury also occur, which lead to mesangial contraction and cessation of glomerular filtration. Therefore, the pathogenesis of acute ischemic renal failure was caused by the interaction of microvascular and tubular events [4, 5].

TGF-β1 (transforming growth factor-β1), an important member of TGF super-family, has identified as the important mediator of renal fibrosis and inflammation associated with multiple progressive kidney diseases [6, 7]. Fibrosis represents the last step of renal injury which eventually leads to final-stage kidney failure [8], therefore, controlling TGF-β1 is an important approach to prevent renal injury.

On the other side we were encouraged by the recent report of 7-substituted coumarin derivatives as COX-2 inhibitors [9]. After this result we wish to test these compounds against acute renal injury, such as renal I/R injury. In the present study, we administered 7-substituted coumarin derivatives to renal I/R injured rats. The injury-induced tubular lesions, renal dysfunction, renal cell apoptosis, alterations in histone methylation and histone methyltransferase/demethylase, as well as the levels of Tgf-β1 were analyzed.

In this paper we revealed the synthesis and potential effects of N-substituted 2-(2-oxo-2H-chromen-4-yloxy)propanamide derivatives for the inhibition of acute renal injury by controlling TGF-β1 in vivo.

Materials and methods

Chemistry

Reagents and Chemicals were purchased from Sigma-Aldrich, and all reagents were of analytical reagent grade. Thin-layer chromatography (TLC) was performed on Merck silica gel 60 F_{254} plates and visualized under UV light. ^{1}H NMR spectra were recorded with Varian Mercury Plus 400 MHz instrument. ^{13}C NMR spectra were recorded with a Varian Gemini 100 MHz instrument. All the chemical shifts are reported in (ppm) using TMS as an internal standard. Multiplicity is indicated by one or more of the following abbreviations: s (singlet), d (doublet), t (triplet), q (quartet), m (multiplet), br (broad); the coupling constants (J) correspond to the order of the multiplicity assignment. Mass spectra were recorded with a PE Sciex model API 3000 instrument. All the reactions were carried out under nitrogen atmosphere.

General procedure for the synthesis of N-substituted-2-(2-oxo-2H-chromen-4-yloxy) propanamide C

The synthesis of N-substituted-2-(2-oxo-2H-chromen-4-yloxy)propanamide C is shown in **Scheme 1**. 2-[(2-Oxo-2*H*-chromen-7-yl)oxy]propanoic acid 4 (1 mmol), amine (1.1 mmol), HBTU (1.1 mmol) in DMF (3 mL) were stirred at room temparature for 4 h. After completion of the reaction water (10 mL) was added to the reaction mixture. The solid separated was filtered and dried to give the desired product.

N-(3-chloro-2-methylphenyl)-2-(2-oxo-2H-chromen-4-yloxy)propanamide (C1)

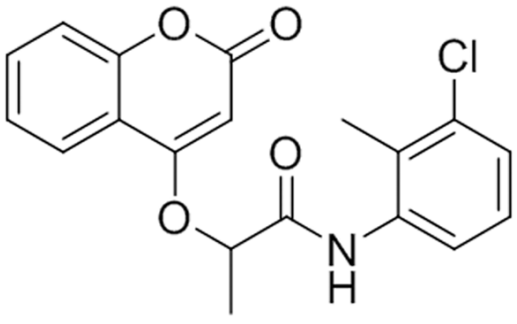

White solid, m.p. 231-233°C; ^{1}H NMR (400 MHz, DMSO-d_6): δ 10.09 (s, 1H), 7.97 (d, *J* = 7.8 Hz, 1H), 7.68 (t, *J* = 6.3 Hz, 1H), 7.42-7.50 (m, 3H), 7.26-7.33 (m, 2H), 5.86 (s, 1H), 5.32 (t, *J* = 6.9 Hz, 1H), 2.21 (s, 3H), 1.72 (d, *J* = 6.5 Hz, 3H); ^{13}C NMR (100 MHz, DMSO-d_6): δ 167.8, 163.7, 161.5, 152.4, 135.5, 133.7, 131.6, 130.3, 125.6, 123.5, 123.1, 122.6, 115.4 (2C), 114.5, 90.5, 74.5, 17.7, 14.1; EI-MS: m/z 358.2 (M+1, 100%).

N-benzyl-2-(2-oxo-2H-chromen-4-yloxy)propanamide (C2)

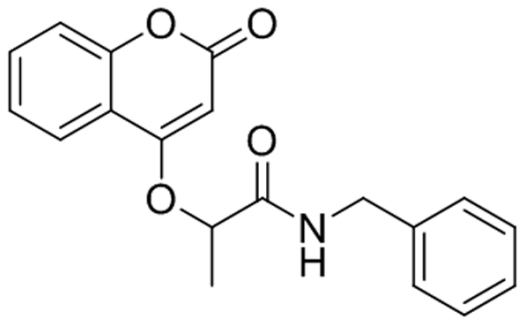

White solid, m.p. 154-156°C; ^{1}H NMR (400 MHz, DMSO-d_6): δ 8.83 (s, 1H), 7.93 (t, *J* = 7.8 Hz, 1H), 7.69 (t, *J* = 6.3 Hz, 1H), 7.43-7.36 (m, 2H), 7.34-7.18 (m, 5H), 5.76 (s, 1H), 5.12 (d, *J* = 6.7 Hz, 1H), 4.32 (s, 2H), 1.63 (d, *J* = 6.6 Hz, 3H); ^{13}C NMR (100 MHz, DMSO-d_6): δ 169.4, 163.8, 162.3, 153.4, 137.5, 132.8, 128.9 (2C), 127.8, 127.6, 124.4, 122.7, 116.8, 115.3, 92.2, 43.3, 18.4; EI-MS: m/z 324.2 (M+1, 100%).

N-(2,4-difluorophenyl)-2-(2-oxo-2H-chromen-4-yloxy)propanamide (C3)

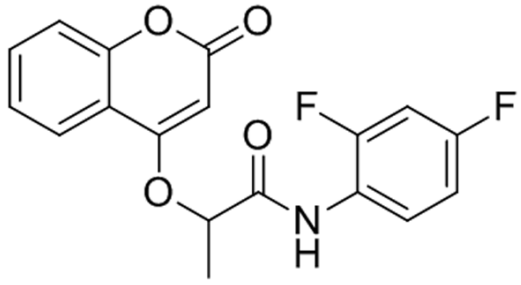

White solid, m.p. 213-215°C; 1H NMR (400 MHz, DMSO-d_6): δ 10.15 (s, 1H), 7.99 (d, *J* = 8.1 Hz, 1H), 7.76-7.66 (m, 2H), 7.43-7.29 (m, 3H), 7.08 (d, *J* = 6.2 Hz, 1H), 5.78 (s, 1H), 5.35 (d, *J* = 6.7 Hz, 1H), 1.69 (d, *J* = 6.7 Hz, 3H); ^{13}C NMR (100 MHz, DMSO-d_6): δ 167.5, 163.4,161.8, 153.5, 133.1, 124.5, 122.9, 122.8, 122.4,

117.4, 115.1, 111.7, 111.5, 103.8, 103.6, 92.5, 75.7, 17.9; EI-MS: m/z 346.2 (M+1, 100%).

N-(4-methoxyphenyl)-2-(2-oxo-2H-chromen-4-yloxy)propanamide (C4)

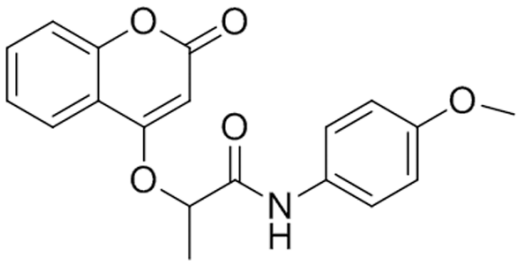

White solid, m.p. 181-183°C; ^{1}H NMR (400 MHz, DMSO-d_6): δ 7.88 (d, *J* = 8.2 Hz, 1H), 7.77 (s, 1H), 7.63 (t, *J* = 7.5 Hz, 1H), 7.42-7.33 (m, 4H), 6.89 (d, *J* = 8.6 Hz, 2H), 5.77 (s, 1H), 4.97 (s, 1H), 3.78 (s, 3H), 1.82 (d, *J* = 6.8 Hz, 3H); ^{13}C NMR (100 MHz, DMSO-d_6): δ166.7, 164.4, 162.7, 153.4, 132.6, 123.8, 123.3, 116.7 (2C), 115.5, 91.3, 72.8, 46.3, 43.6, 29.7, 26.5, 25.5, 24.3, 17.5; EI-MS: m/z 340.2 (M+1, 100%).

4-(1-Morpholino-1-oxopropan-2-yloxy)-2H-chromen-2-one (C5)

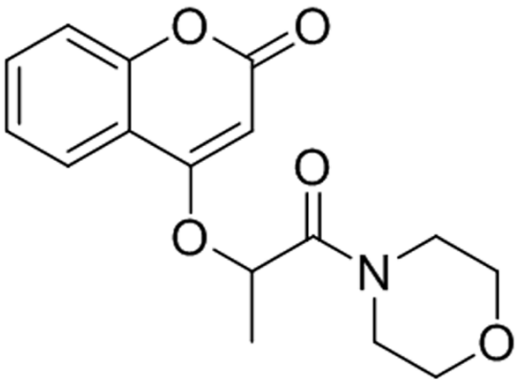

Brown solid, m.p. 137-140°C; ^{1}H NMR (400 MHz, DMSO-d_6): δ 7.87 (d, *J* = 7.8 Hz, 1H), 7.69 (t, *J* = 6.3 Hz, 1H), 7.43-7.38 (m, 2H), 5.72 (s, 1H), 5.64 (d, *J* = 6.6 Hz, 1H), 3.63-3.39 (m, 8H), 1.57 (d, *J* = 6.6Hz, 3H); ^{13}C NMR (100 MHz, DMSO-d_6): δ 167.2, 164.2, 162.5, 153.4, 132.8, 124.2, 123.1, 116.8, 115.3, 91.5, 73.1, 66.9, 66.5, 45.8, 42.7, 17.3; EI-MS: m/z 304.1 (M+1, 100%).

4-(1-Oxo-1-(pyrrolidin-1-yl)propan-2-yloxy)-2H-chromen-2-one (C6)

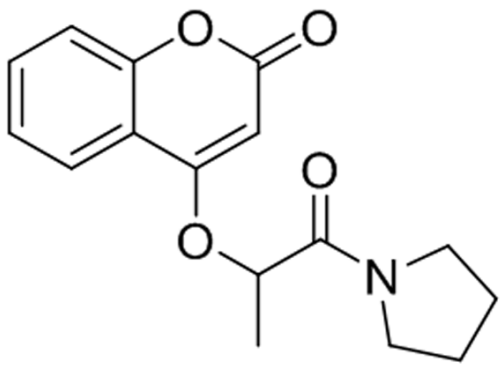

Brown solid, m.p. 177-179°C; ^{1}H NMR (400 MHz, DMSO-d_6): δ7.87 (d, *J* = 8.2 Hz, 1H), 7.68 (dd, *J* = 11.4, 4.3 Hz, 1H), 7.47-7.35 (m, 2H), 5.35 (q, *J* = 6.4 Hz, 1H), 5.64 (s, 1H), 3.67 (t, *J* = 6.2 Hz, 1H), 3.39-3.33 (m, 3H), 1.87-1.81 (m, 2H), 1.78-1.75 (m, 2H), 1.58 (d, *J* = 6.6 Hz, 3H); ^{13}C NMR (100 MHz, DMSO-d_6): δ166.8, 164.4, 162.5, 153.4, 132.6, 123.8, 123.3, 116.5, 115.5, 91.4, 73.6, 46.6, 46.1, 26.4, 23.5, 16.8; EI-MS: m/z 288.2 (M+1, 100%).

N-(2-cyano-4-(trifluoromethyl)phenyl)-2-(2-oxo-2H-chromen-4-yloxy)propanamide (C7)

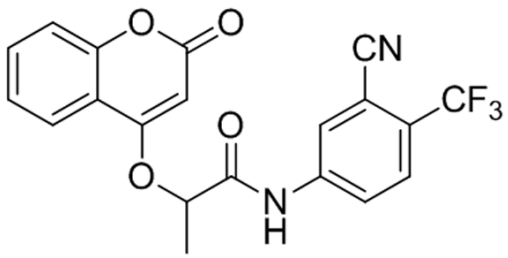

Brown solid, m.p. 262-265°C; ^{1}H NMR (400 MHz, DMSO-d_6): δ 10.87 (s, 1H), 8.25 (s, 1H), 8.08 (d, *J* = 4.9 Hz, 1H), 7.97 (dd, *J* = 7.8, 2.6 Hz, 1H), 7.87 (d, *J* = 8.6 Hz, 1H), 7.62 (d, *J* = 7.4 Hz, 1H), 7.36-7.43 (m, 2H), 5.73 (s, 1H), 5.16 (d, *J* = 6.8 Hz, 1H), 1.77 (d, *J* = 6.8 Hz, 3H); ^{13}C NMR (100 MHz, DMSO-d_6): δ 167.8, 163.1, 160.9, 152.0, 141.5, 134.6, 131.5, 122.8, 122.5,

122.3, 121.3, 116.4, 116.5, 115.2, 114.4, 114.1, 102.3, 90.2,73.5, 17.3; EI-MS: m/z 401.1 (M-1, 100%).

Methyl 4-methyl-2-(2-(2-oxo-2H-chromen-4-yloxy)propanamido)pentanoate (C8)

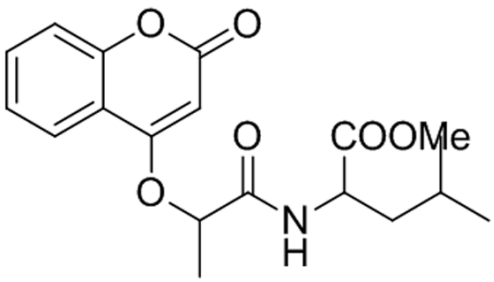

White solid; 186-188°C; ^{1}H NMR (400 MHz, $CDCl_3$): δ 7.88 (t, *J* = 8.8 Hz, 2H), 7.53-7.64 (m, 2H), 7.28- 7.38 (m, 4H), 6.79 (d, *J* = 8.2 Hz, 2H), 5.74 (d, *J* = 1.3 Hz, 2H), 4.92 (dd, *J* = 14.3, 2H), 4.68 (dd, *J* = 8.2, 2H), 3.78 (s, 3H), 3.72 (s, 3H), 1.43-1.58 (m, 7H), 1.02-0.95 (m, 6H), 0.89 (dd, *J* = 8.2, 12H); ^{13}C NMR (100 MHz, DMSO-d_6): δ 167.2, 163.8, 162.5, 156.8, 153.4, 132.8, 129.6, 124.3, 122.8, 122.3, 116.8 (2C), 115.3, 114.3, 92.2, 75.9, 55.5 (2C), 18.2; EI-MS: m/z 362.1 (M+1, 100%).

N-(1-oxo-1,2-dihydroisoquinolin-5-yl)-2-(2-oxo-2H-chromen-4-yloxy)propanamide (C9)

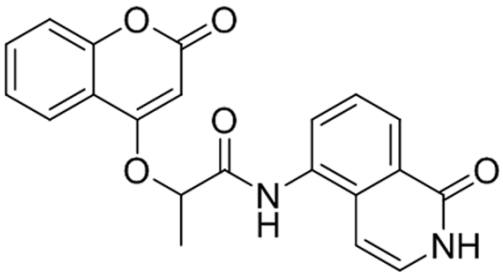

White solid, m.p. 192-194 °C; ^{1}H NMR (400 MHz, DMSO-d_6): δ 8.07 (s, 2H), 7.92 (d, *J* = 7.4 Hz, 1H), 7.85-7.78 (m, 2H), 7.71 (s, 1H), 7.64 (dd, *J* = 11.2, 4.0 Hz, 1H), 7.45 (t, *J* = 7.9 Hz, 1H), 7.38 (t, *J* = 7.8 Hz, 2H), 7.24 (d, *J* = 7.2 Hz, 1H), 5.80 (s, 1H), 5.04 (q, *J* = 6.2 Hz, 1H), 1.82 (d, *J* = 6.7 Hz, 3H); ^{13}C NMR (100 MHz, DMSO-d_6): δ 167.8, 164.1, 162.7, 161.4, 153.4, 139.4, 137.8, 132.8, 129.9 (2C), 126.8 (2C), 124.4, 122.8, 118.1, 116.8 (2C), 115.3, 92.2, 29.7, 18.2; EI-MS: m/z 377.2 (M+1, 100%).

2-(2-Oxo-2H-chromen-4-yloxy)-N-(4-(3-oxomorpholino)phenyl)propanamide (C10)

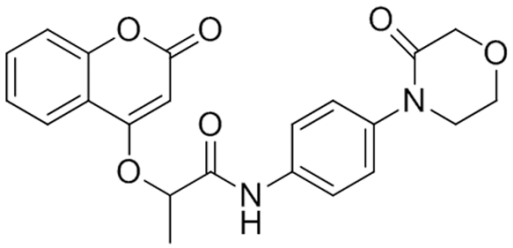

Brown solid, m.p. 152-154°C; ^{1}H NMR (400 MHz, DMSO-d_6): δ 8.56 (s, 1H), 7.94 (d, *J* = 6.8 Hz, 1H), 7.58-7.61 (m, 1H), 7.48 (d, *J* = 8.8 Hz, 2H), 7.34 (t, *J* = 7.4 Hz, 2H), 7.26 (d, *J* = 6.0 Hz, 2H), 5.68 (s, 1H), 4.98 (q, 1H), 4.32 (s, 2H), 4.04 (t, 2H), 3.78 (t, *J* = 4.8 Hz, 2H), 1.78 (d, *J* = 6.6 Hz, 3H); ^{13}C NMR (100 MHz, DMSO-d_6): δ 167.7, 167.2, 164.2, 162.5, 153.5, 137.7, 135.8, 132.8, 126.2, 124.3, 123.1, 122.8, 121.4 (2C), 115.4, 92.2, 75.6, 68.5, 64.1, 49.9, 18.2 (2C); EI-MS: m/z 409.2 (M+1, 100%).

2-(2-Oxo-2H-chromen-4-yloxy)-N-(pyridin-4-yl) propanamide (C11)

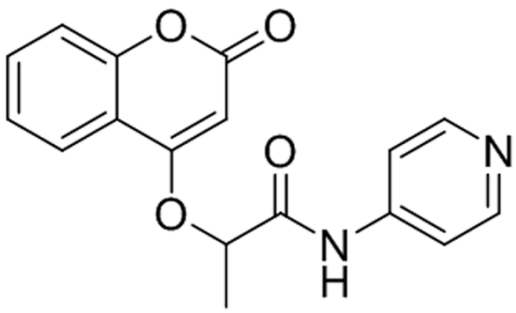

Off white solid, m.p. 199-201°C; ^{1}H NMR (400 MHz, DMSO-d_6): δ10.12 (s, 1H), 8.24 (d, *J* = 4.8 Hz, 2H), 7.76 (dd, *J* = 7.8, 2.4 Hz, 1H), 7.43-7.32 (m, 3H), 7.12 (q, *J* = 6.4 Hz, 2H), 5.48 (s, 1H), 4.87 (q, *J* = 6.2 Hz, 1H), 1.57 (d, *J* = 6.6 Hz, 3H); ^{13}C NMR (100 MHz, DMSO-d_6): δ 168.8, 164.4, 162.4, 153.2, 149.8 (2C), 145.6, 132.6, 123.8, 123.4, 116.4 (2C), 115.3, 114.1, 91.2, 74.5, 18.2; EI-MS: m/z 310.9 (M+1, 100%).

Biology

Animals and renal ischemia/reperfusion (I/R) model: Male Wistar rats were housed in ventilated micro isolator cages with free access to water and food. Rats weighing 160 ± 20 g were

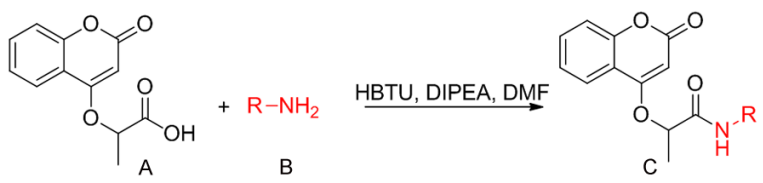

Scheme 1. Synthetic scheme of N-substituted-2-(2-oxo-2H-chromen-4-yloxy) propanamide (C).

used and assigned to one of the following groups: CT group, uninjured rats with vehicle administration; I/R group, rats underwent I/R injury with vehicle administration; I/R + C7 group, rats underwent I/R injury with 5 μg/kg BW C7 administered twice per day. C7 was chemically synthesized from the literature known method [Rambabu et al.]. I/R injury was performed as previously reported [10]. In brief, rats were anesthetized and underwent incisions at midline abdominal with their left renal pedicle openly clamped by a clamp for 30 min. After removing the clamps, wounds were sutured and the animals were allowed to recover for 3 days before sacrifice. Control animals were sham operated. All animal experiments were approved by the Committee on Ethics in the Care.

Assessment of renal function: Urine samples of the animals were collected for 24 h in metabolic cages 1 day before sacrifice. Total protein and creatinine in urine levels were measured with an Olympus AU2700 automatic biochemistry analyzer using a creatinine reagent kit (Fuxing Changzheng Medical Inc., Shanghai, China) as described in the literature [11].

Renal histology: Hematoxylin and eosin (H&E) was used to stain the renal sections. Hallmarks of acute tubular necrosis (ATN) were examined on a double-blind basis. The percentage of renal damage was evaluated semi-quantitatively with a scale in which 0 represents no abnormalities, and 1+, 2+, 3+, 4+ stand for slight (up to 20%), moderate (20 to 40%), severe (40 to 60%), and total necrosis (affecting more than 80% of renal parenchyma), respectively [12].

TUNEL assay: Paraffin-embedded sections were deparaffinized and rehydrated as reported [13]. TUNEL assay was used to detect the apoptotic cells using an In Situ Cell Death Detection Kit (Roche, Mannheim, Germany) [14]. At least six different areas per renal sample of TUNEL positive cells were counted using an Olympus BX60 microscope equipped with a digital CCD and reported as number of TUNEL-positive nuclei divided by the total number of cells per field.

In vitro H/R injury and cell culture: In *vitro* H/R experiments referred to a literature report [14]. At 80% confluence, cells were put into a 37°C incubator under 1% O_2 with the normal media replaced with media lacking glucose and FBS, which was regarded as hypoxia. After culturing under the hypoxia condition for a specified amount of time (4 hrs for HBZY-1 cells and 1 hr for NRK-52E cells), cells were returned to the normal culture condition for two hours, which was regarded as reperfusion. For C7 treatment, 300 pM C7 was added to media during the hypoxia and reperfusion period. 2-TCP (trans-2-Phenylcyclopropylamine hydrochloride), a HDM inhibitor [15], was added to media to induce the total methylation of H3K4 in the cultured renal cells.

NRK-52E (a rat tubular epithelia cell line) and HBZY-1 (a rat mesangial cell line) were cultured in DMEM media with 5.5 mM glucose plus 5% fetal bovine serum (FBS) (Gibco, Grand Island, USA), and maintained in a 37°C incubator (Thermo scientific, Marietta, USA) with humidified atmosphere of 21% O_2 which was regarded as the normal culture condition.

Transfection: HBZY-1 cells were plated in six-well plates and transfected the next day with either pPCAGSIH-β-gal or pPCAGSIH-C7 plasmids using Fugene HD transfection reagent (Promega, Madison, USA) according to the manufacturer's instruction.

Western blots: Freshly collected kidney or cultured cells were sonicated in ice-cold RIPA buffer (Beyotime, Haimen, China) and protein concentrations were quantitated as previously described [16]. For immunodetection, 20-80 μg of protein from each sample were separated and transferred onto PVDF membranes. The intensity of the required protein bands were evaluated using Quantity One 1-D Analysis Software. Individual protein levels were quantitated relative to the β-actin level in the same

Table 1. Synthesis of a novel series of N-substituted-2-(2-oxo-2H-chromen-4-loxy) propanamide (C)[a]

Entry	Amine (2)	Product	Yield (%)
1	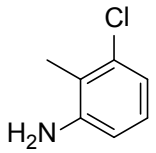	C1	82
2	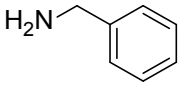	C2	83
3	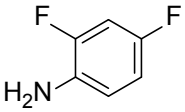	C3	81
4	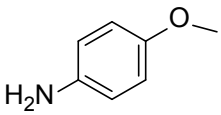	C4	78
5	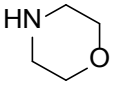	C5	84
6		C6	87
7	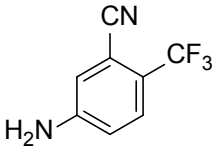	C7	82
8	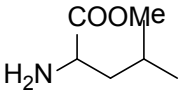	C8	85
9	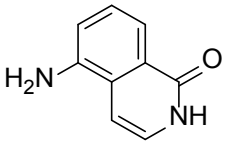	C9	92
10	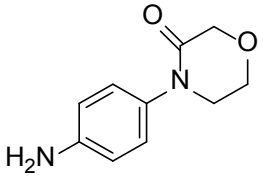	C10	96

Note: [a]isolated yields.

sample and further normalized to the respective control group, which was set at one.

RNA isolation and RT-PCR: RNA[iso] Plus (TaKaRa Biotechnology, Dalian, China) was used to isolate the Total RNA from kidneys or cultured cells. M-MLV first strand synthesis system (Invitrogen, Grand Island, USA) was used to reverse transcribe the total RNA into cDNA. PCR was used to find the abundance of specific gene transcripts. PCR products were separated by electrophoresis using 1.5% agarose gels, and Molecular Imager Gel Doc XR (Bio-Rad, Hercules, USA) was used to take the images. Quantity One 1-D Analysis Software (Bio-Rad) was used to quantify the band density. The mRNA level of the targeted gene was quantitated first against the *Rn18s* level from the same sample, then normalized to the non-injured group or the cells transferred with pPCAGSIH-β-gal under normal conditions, which was set at one.

Chromatin immunoprecipitation (ChIP) assay: Kidneys were cross-linked with 1% formaldehyde for 10 min and a ChIP assay was performed. Chromatin was immunoprecipitated with an anti-H3K4me2 antibody (Abcam, Cambridge, UK). The purified DNA was detected by PCR. The input samples were used as an internal control for comparison between samples.

Statistical analysis

The data were expressed as mean ± standard error of the mean (SEM). Statistical significance was determined by analyzing the data with the non parametric Kruskal-Wallis test, followed by the Mann-Whitney test. Differences were considered statistically significant at $P < 0.05$.

Results and discussion

Chemistry

To find the optimum reaction condition, the reaction of 2-(2-oxo-2H-chromen-4-yloxy)propanoic acid (A), with amine (B) in DMF using HBTU was carried out at room temperature for 10-12 h which yielded N-substituted-2-(2-oxo-2H-chromen-4-yloxy)propanamide (C) in more than 80% yield (**Table 1**, entry 1). Several amines were used for checking the compatibility of this reaction. All the amines including aromatic and aliphatic amines were well tolerated with the current reaction to yield the required products in good to excellent yields. Thus, the structures of the synthesized compounds are shown in **Table 1**.

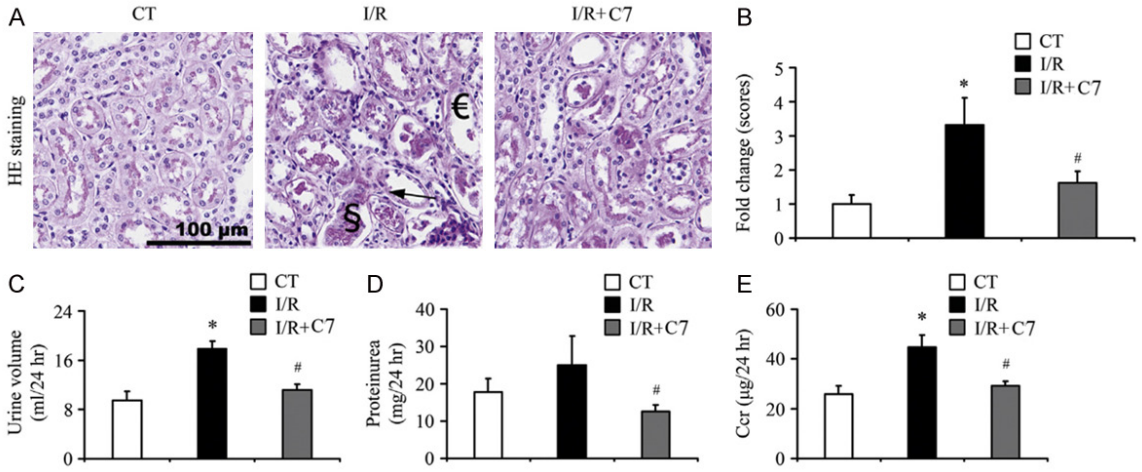

Figure 1. C7 treatment inhibits I/R injury induced renal dysfunction. Representative HE staining pictures (A) and quantitative results of renal damage score (B) in different experimental groups. (C) Urine volume in different experimental groups. (D) Proteinuria in different experimental groups. (E) Urine creatinine concentration in different experimental groups. CT, non-injured rats; I/R, I/R injured rats; I/R + C7, C7 treated I/R injured rats, n = 5-7 per group. § indicates vast formation; arrow indicates tubular cells denudation; € indicates tubular necrosis. *p b 0.05 compared to CT rats; #P b 0.05 compared to I/R injured rats.

Biological evaluation

C7 protects against renal I/R injury induced morphological changes: The effects of C7 on the renal morphological changes at different dosages (2, 5, 10 and 15 μg/kg BW) were examined after 3 days of I/R injury. The I/R injuried kidney presented severe tubular damage, as evidenced by widespread tubular necrosis, cast formation and tubular cells denudation (**Figure 1A**). Histochemistry results showed that administration of 10 and 15 μg/kg BW of C7 has protective effects on renal morphology, while lower doses (2 or 5 μg/kg BW) showed no obvious beneficial effects on renal morphology after the I/R injury.

Using of 10 μg/kg C7 treatment significantly improved the pathological scores in the injured kidneys (**Figure 1B**); so this dose was chosen for further in vivo experiments. Kidney damage was estimated by measurement of 24 h urine volume, proteinuria and urine creatinine concentration. Functional renal studies demonstrated that renal I/R injury caused kidney dysfunction, as reflected by significantly elevated 24 h urine volume, proteinuria and urine creatinine (**Figure 1C-E**); whereas C7 treatment suppressed I/R injury induced elevation of these renal function parameters (**Figure 1C-E**).

C7 normalizes I/R or H/R injury induced down-regulation of Apln mRNA level in vivo and in vitro: The Apln mRNA level was examined in different experimental groups. As estimated, the mRNA level of Apln was significantly lowered in the kidney after I/R injury, while the administration of C7was largely prevented this injury (**Figure 2A**). At the same time, the protein level of APJ, the endogenous receptor for C7, was similar among three groups. Hypoxia inducible factor 1α (Hif1α), a key factor involved in the cellular and systemic responses to hypoxia, has been demonstrated to contribute to the pathogenesis of I/R injury [17].

After I/R injury, the protein level of Hif1α was increased in the kidneys, whereas administration of C7 significantly reduced I/R injury-induced up-regulation of Hif1α (**Figure 2B**).

NRK-52E cells and HBZY-1 cells were used to find the effects of C7 treatment under in vitro H/R condition. A known hypoxia sensor, the levels of Hif1α markedly increased after H/R injury in both the cells (**Figure 2D** and **2F**), indicating the successful establishment of hypoxic injury in these cells.

In NRK-52E cells, H/R led to a significant decrease in Apln mRNA level. The injury-induced decrease in Apln mRNA was significantly inhibited by administrating C7 to the injured renal tubular epithelial cells (**Figure 2C**). There was no significant change in the APJ protein level among the three groups (**Figure 2D**). Similar to what we found in NRK-52E cells, the Apln mRNA level was also signifi-

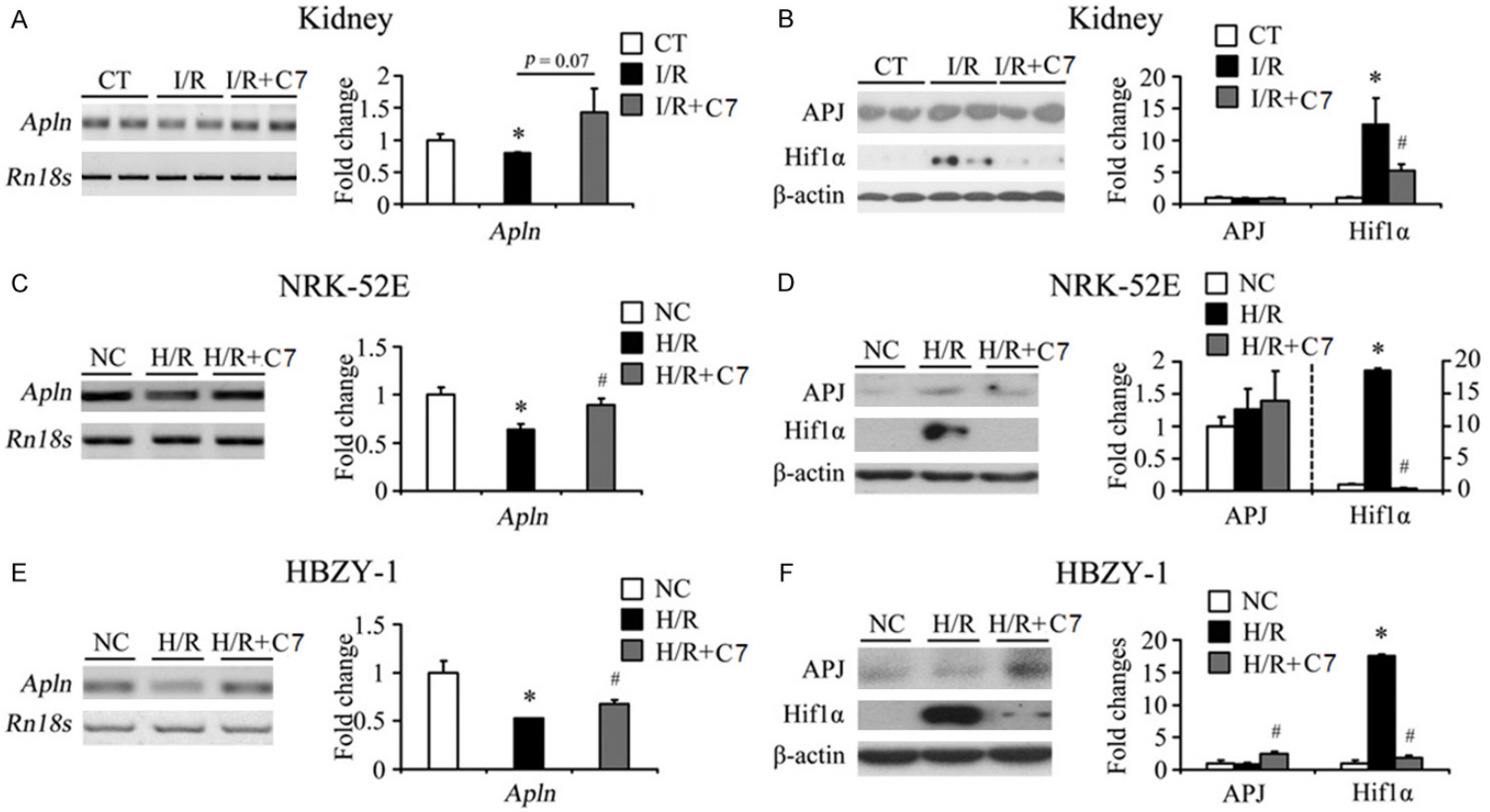

Figure 2. C7 normalized I/R or H/R injury induced downregulation of Apln mRNA level and Hif1α overexpression in kidneys, cultured renal cells. Representative PCR analysis with densitometric quantitative results of Apln, Rn18s were shown in (A, C, E). Representative Western blot analysis with densitometric quantitative results of APJ, Hif1α and β-actin were shown in (B, D, F). CT or NC, non-injured rats or cells; I/R or H/R, I/R injured rats or H/R injured cells; I/R or H/R + C7, C7-13 treated I/R injured rats or H/R injured cells, n = 3-5 per group. *p b 0.05 compared to CT or NC group; #p b 0.05 compared to I/R or H/R group.

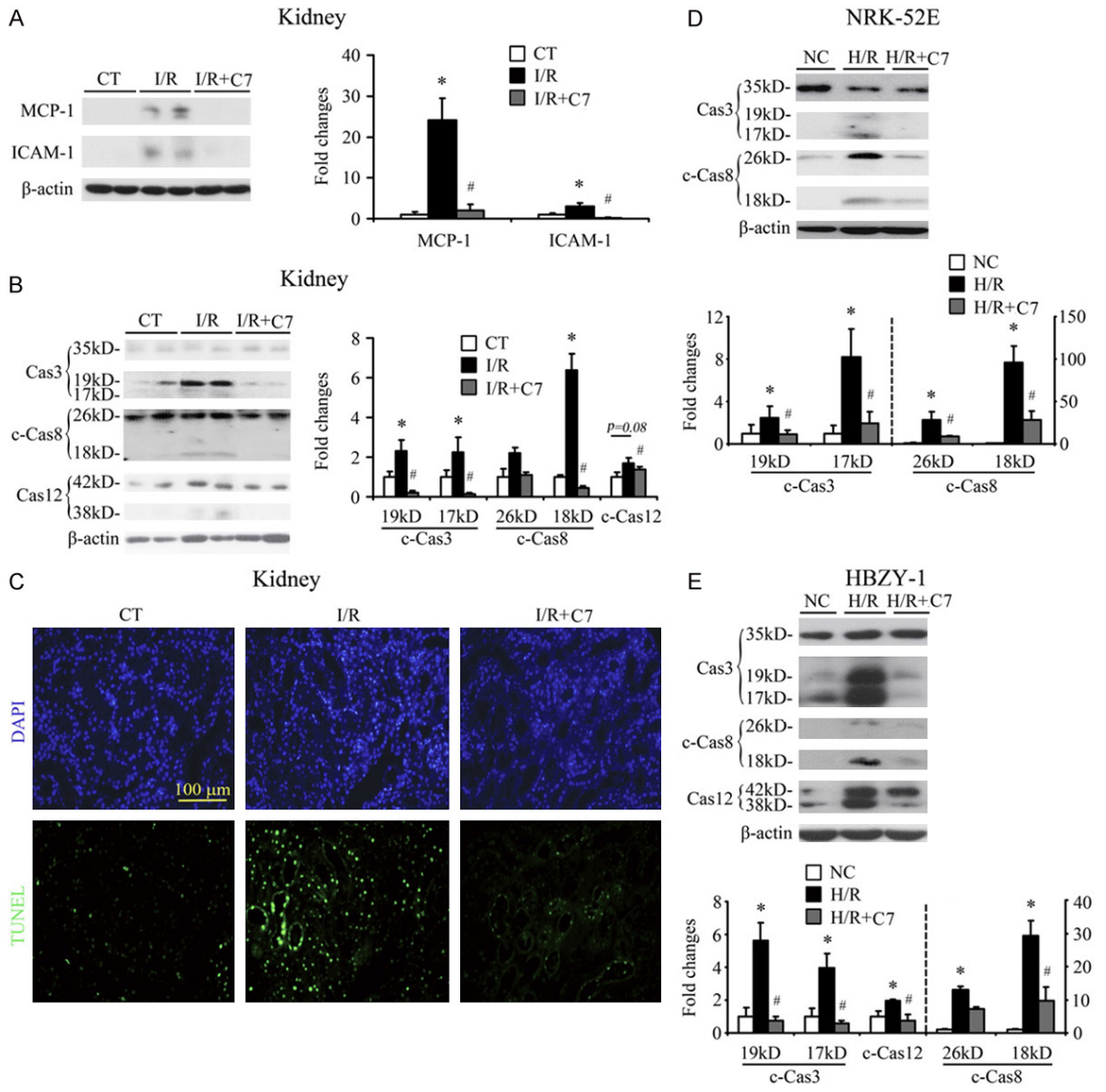

Figure 3. C7 suppresses I/R or H/R injury induced inflammation and apoptosis in kidneys, cultured renal cells. RepresentativeWestern blot analysis with densitometric quantitative results of MCP-1, ICAM-1 and β-actin were shown in (A). Representative Western blot analysis with densitometric quantitative results of caspase-3 (35 KD), c-cas3 (19 KD), c-cas3 (17 KD), c-cas8 (26 KD), c-cas8 (18 KD), caspase12 (42 KD), c-cas12 (38 KD), and β-actin are shown in (B, D and E). (C) Representative TUNEL stained pictures for different experimental groups. Top panels, DAPI staining (blue color); bottom panels, TUNEL staining (green color). CT or NC, non-injured rats or cells; I/R or H/R, I/R injured rats or H/R injured cells; I/R or H/R + C7, C7 treated I/R injured rats or H/R injured cells, n = 3-7 per group. *p b 0.05 compared to CT or NC group; #p b 0.05 compared to I/R or H/R group.

cantly decreased under an H/R condition, which was markedly up-regulated by C7 treatment in the injured HBZY-1 cells (**Figure 2E**). Furthermore, C7 treatment normalized the injury-induced elevation of Hif1α level in both cell lines (**Figure 2D** and **2F**).

C7 suppresses I/R or H/R injury induced inflammation and apoptosis: Up-regulation of inflammatory chemokines and adhesion molecules in the injured sites causes inflammatory cells to infiltrate, which in turn amplifies I/R injury [18, 19]. We found that the levels of MCP-1 (an inflammatory chemokine) and ICAM-1 (an adhesion molecule) were both significantly induced in the kidneys after renal I/R injury.

Treatment with C7 significantly reduced the injury-induced upregulation of ICAM-1 and

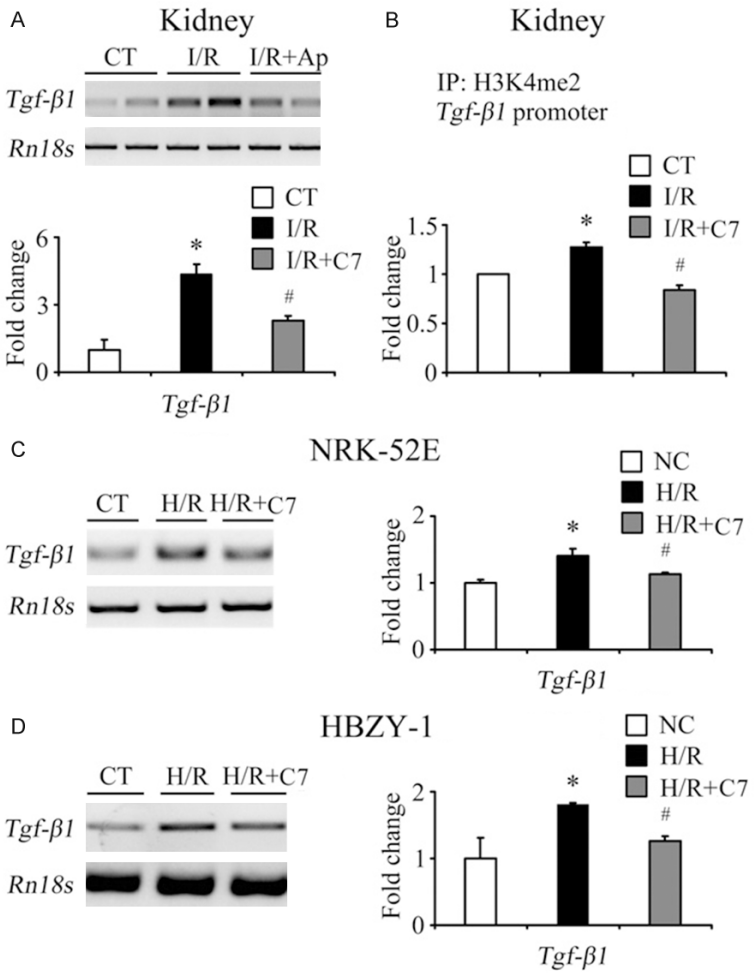

Figure 4. C7 inhibits I/R or H/R injury induced Tgf-β1 in kidneys and cultured renal cells. Representative PCR analysis with densitometric quantitative results of Tgf-β1 and Rn18s are shown in (A, C, D). (B) Quantitative analysis of PCR of chromatin immunoprecipitated DNA, which measures the binding affinity of H3K4me2 to the promoter of Tgf-β1. The abundance is relative to the input in the same sample with the same primer. CT or NC, non-injured rats or cells; I/R or H/R, I/R injured rats or H/R injured cells; I/R or H/R + C7, C7 treated I/R injured rats or H/R injured cells, n = 3 per group. *p b 0.05 compared to NC group; #p b 0.05 compared to I/R or H/R group.

MCP-1 in the kidneys (**Figure 3A**). Cleavage of caspase-3 and caspase-8 activates these two caspases and represents the execution stage of cell death [20]. When compared to the non-injured kidneys, elevation of the cleaved, active forms of caspase-3 and caspase-8 were found in the kidneys of I/R injured rats.

Administration of C7 markedly decreased such injury-induced activation of caspases (**Figure 3B**). Compared to the non-injured kidneys, there was a trend toward elevation of cleaved forms of caspase-12 in the kidneys of I/R injured rats, while administration of C7 significantly inhibited the cleavage of caspase-12 compared to the I/R-injury (**Figure 3B**). A further study to determine whether C7 treatment inhibits I/R injury-induced apoptosis in the kidneys, a TUNEL assay was performed. Substantially increased numbers of TUNEL+ cells were evident in renal tubular cells after the injury, while treatment with C7 significantly abrogated such injury induced increase in cell death (**Figure 3C**).

Similar with the in vivo studies, the levels of the active, cleaved forms of caspase-3 and caspase-8 were also significantly increased in NRK-52E cells in the H/R injury model (**Figure 3D**). Treatment with C7 remarkbly suppressed H/R stimulated activation of cell death (caspase-8 and caspase-3) in cultured renal tubular epithelial cells (**Figure 3D**). Consistent with the results of NRK-52E cells, the levels of active, cleaved forms of caspase-3, caspase-8 and caspase-12 were also significantly increased in HBZY-1 cells following H/R injury (**Figure 3E**). C7 treatment markedly suppressed H/R stimulated activation of cell death in cultured mesangial cells (**Figure 3E**).

C7 inhibits I/R or H/R injury induced up-regulation of Tgf-β1: TGF-β1 has long been implicated as a central mediator of acute renal injury [21]. Significantly increased Tgf-β1 mRNA was evident in the kidneys after I/R injury, and C7 treatment significantly reduced I/R-induced up-regulation of Tgf-β1 in the kidneys (**Figure 4A**). A ChIP assay further demonstrated increased recruitment of H3K4me2 to the promoter of Tgf-β1, which was consistent with

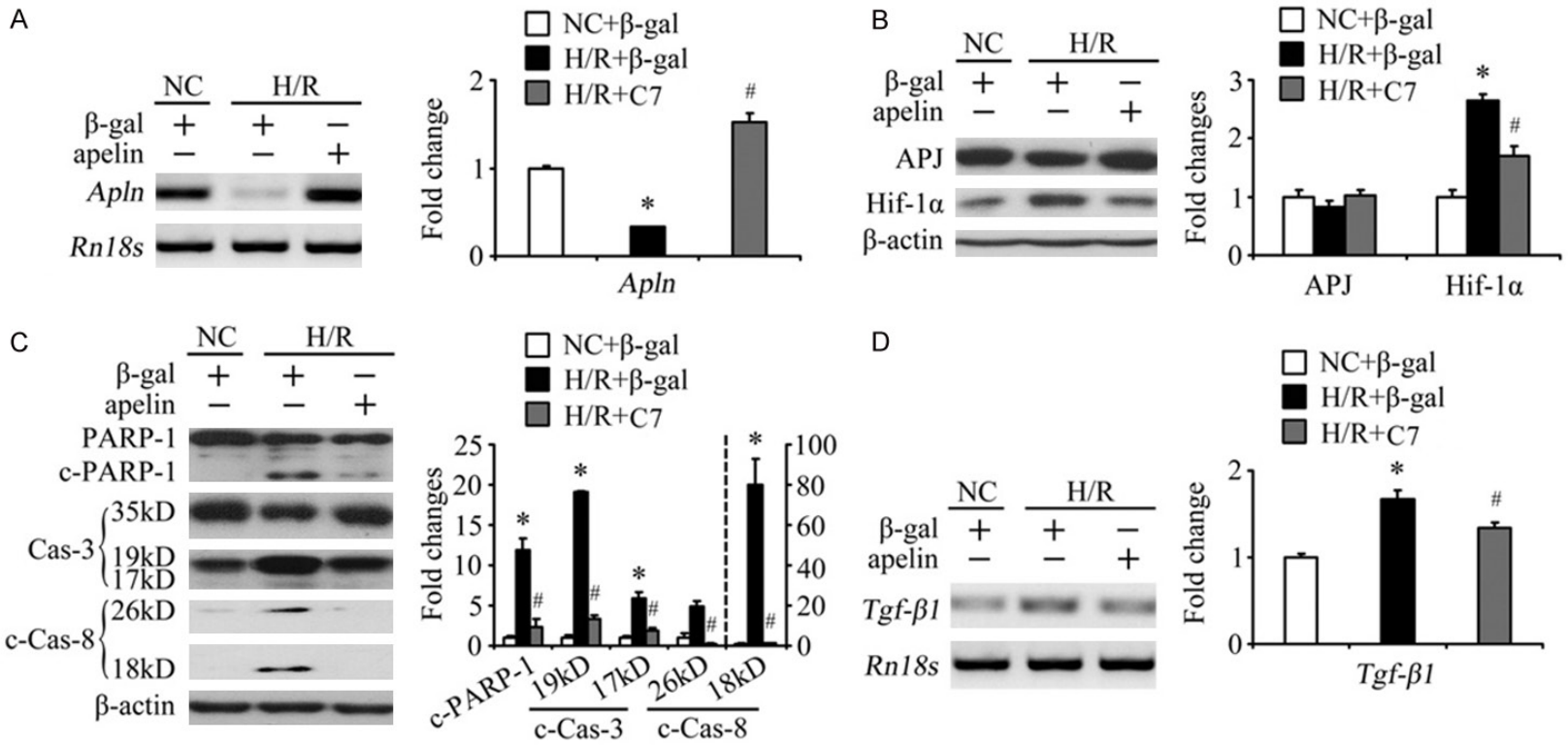

Figure 5. Over-expression of C7 inhibits H/R activated apoptosis and Tgf-β1 in HBZY-1 cells. Representative PCR analysis with densitometric quantitative results of Apln, Rn18s were shown in (A). RepresentativeWestern blot analysiswith densitometric quantitative results of APJ, Hif1α and β-actin were shown in (B). RepresentativeWestern blot analysis with densitometric quantitative results of caspase-3 (35 KD), c-cas3 (19 KD), c-cas3 (17 KD), c-cas8 (26KD), c-cas8 (18KD), PARP-1, c-PARP-1 and β-actinwere shown in (C). Representative PCR analysis with densitometric quantitative results of Tgf-β1 and Rn18s are shown in (D). NC + β-gal, cells transfected with the pPCAGSIH-β-gal plasmid cultured under normal condition; H/R + β-gal, cells transfected with the pPCAGSIH-β-gal plasmid cultured under H/R condition; H/R + apelin, cells transfected with the pPCAGSIH-apelin plasmid cultured under H/R condition, n = 3 per group. *p b 0.05 compared to NC group; #p b 0.05 compared to H/R + β-gal group.

the increased mRNA level of Tgf-β1 found in the kidneys of I/R injured rats. C7 treatment significantly controlled the I/R-induced increase in H3K4me2 binding to the promoter of Tgf-β1 in the kidneys (**Figure 4B**). Consistent with the in vivo study, significantly increased Tgf-β1 mRNA was also observed in tubular epithelial cells and mesangial cultured under H/R conditions, and C7 treatment reduced H/R-induced elevation of Tgf-β1 (**Figure 4C** and **4D**).

Over-expression of C7 protects mesangial cells from H/R induced apoptosis and Tgf-β1 up-regulation: In addition to direct C7 treatment, the pPCAGSIH-C7 plasmid was used to study the effects of C7 over-expression in H/R injured mesangial cells. Apln mRNA was significantly decreased in H/R injured cells compared to control cells. Over-expression of C7 markedly up-regulated Apln mRNA level in HBZY-1 cells cultured under H/R conditions (**Figure 5A**). No significant difference in APJ level was observed in HBZY-1 cells cultured under different conditions. Furthermore, overexpression of apelin significantly suppressed H/R-induced increased Hif1α level in HBZY-1 cells (**Figure 5B**). Caspase-3 has been shown to be primarily responsible for the cleavage of poly(ADP-ribose) polymerase-1 (PARP-1) during cell death [46].

Compared to control cells, elevated cell death in H/R stimulated cells was demonstrated by elevation of the cleaved, active form of caspase-3, caspase-8 and PARP-1, and these changes were markedly attenuated by apelin over-expression (**Figure 5C**).

We next examined whether over-expression of C7 could suppress H/R up-regulated Tgf-β1 mRNA level in HBZY-1 cells. A significant increase of Tgf-β1 mRNA level in HBZY-1 cells after H/R injury was observed, which was markedly suppressed by over-expression of C7 (**Figure 5D**).

Discussion

The number of AKI patientsis increasing worldwide, whereas an optimal therapy for AKI is still lacking [22, 23]. Rodent renal I/R injury is a good model to study the pathogenesis of AKI and to seek possible therapies for the disease.

In the present study, we report that C7 significantly inhibits I/R injury induced renal dysfunction in rats. Furthermore, our results demonstrate that C7 suppressed inflammation (ICAM-1 expression) and apoptosis (caspase-3 activation) in both renal I/R injured rats and renal cells cultured under H/R injury conditions. Thus, our data suggested that C7 plays a protective role in renal I/R injury through its anti-apoptotic and anti-inflammatory action.

In summary, this study revealed a novel mechanism underlying the anti-inflammatory, anti-apoptotic of C7, which confers protection against I/R injury in the kidney by epigenetic regulation. All these findings suggest that C7 may be considered as a viable strategy to prevent acute cell damage and improve the outcome of I/R injury to the kidneys.

Acknowledgements

This study was supported by Science and Technology Program of Jinan City, China (No: 2014jnnk04).

Disclosure of conflict of interest

None.

Address correspondence to: Xin-Jian Li, Department of Nephrology, Affiliated Hospital of Jining Medical College, Jining 272000, Shangdong, China. E-mail: lixinjianxj@hotmail.com

References

[1] Star RA. Treatment of acute renal failure. Kidney Int 1998; 54: 1817-1831.
[2] Gueler F, Gwinner W, Schwarz A, Haller H. Long-term effects of acute ischemia and reperfusion injury. Kidney Int 2004; 66: 523-527.
[3] Schiffl H, Lang SM, Fischer R. Daily hemodialysis and the outcome of acute renal failure. N Engl J Med 2002; 346: 305-310.
[4] Petry C, Huwiler A, Eberhardt W, Kaszkin M, Pfeilschifter J. Hypoxia increases group IIA phospholipase A(2) expression under inflammatory conditions in rat renal mesangial cells. J Am Soc Nephrol 2005; 16: 2897-2905.
[5] Bonventre JV, Weinberg JM. Recent advances in the pathophysiology of ischemic acute renal failure. J Am Soc Nephrol 2003; 14: 2199-2210.
[6] Border WA, Noble NA. Transforming growth factor beta in tissue fibrosis. N Engl J Med 1994; 331: 1286-1292.
[7] Choi ME, Ding Y, Kim SI. TGF-beta signaling via TAK1 pathway: role in kidney fibrosis. Semin Nephrol 2012; 32: 244-252.

[8] Becker S, Walter S, Witzke O, Kreuter A, Kribben A, Mitchell A. Application of gadolinium-based contrast agents and prevalence of nephrogenic systemic fibrosis in a cohort of end-stage renal disease patients on hemodialysis. Nephron Clin Pract 2012; 12: c91-c94.
[9] Rambabu D, Mulakayala N, Ismail, Ravi Kumar K, Pavan Kumar G, Mulakayala C, Kumar CS, Kalle AM, Basaveswara Rao MV, Oruganti S, Pal M. Synthesis and pharmacological evaluation of N-substituted 2-(2-oxo-2H-chromen-4-yloxy)propanamide as cyclooxygenase inhibitors. Bioorg Med Chem Lett 2012; 22: 6745-6749.
[10] Supavekin S, Zhang W, Kucherlapati R, Kaskel FJ, Moore LC, Devarajan P. Differential gene expression following early renal ischemia/reperfusion. Kidney Int 2003; 63: 1714-1724.
[11] Chen H, Li J, Jiao L, Petersen RB, Peng A, Zheng L, Huang K. Apelin inhibits the development of diabetic nephropathy by regulating histone acetylation in Akita mouse. J Physiol 2014; 592: 505-521.
[12] Dragun D, Hoff U, Park JK, Qun Y, Schneider W, Luft FC, Haller H. Prolonged cold preservation augments vascular injury independent of renal transplant immunogenicity and function. Kidney Int 2001; 60: 1173-1181.
[13] Wang LL, Chen H, Huang K, Zheng L. Elevated histone acetylations in Muller cells contribute to inflammation: a novel inhibitory effect of minocycline. Glia 2012; 60: 1896-1905.
[14] Wang Y, Li R, Qiao X, Tian J, Su X, Wu R, Zhang R, Zhou X, Li J, Shao S. Intermedin/adrenomedullin 2 protects against tubular cell hypoxia-reoxygenation injury in vitro by promoting cell proliferation and upregulating cyclin D1 expression. Nephrology (Carlton) 2013; 18: 623-632.
[15] Min Gyu Lee CW, Schmidt DM, McCafferty DG, Shiekhattar R. Histone H3 lysine 4 demethylation is a target of nonselective antidepressive medications. Chem Biol 2006; 13: 563-567.
[16] Chen H, Zheng C, Zhang X, Li J, Zheng L, Huang K. Apelin alleviates diabetesassociated endoplasmic reticulum stress in the pancreas of Akita mice. Peptides 2011; 32: 1634-1639.
[17] Haase VH. Pathophysiological consequences of HIF activation: HIF as a modulator of fibrosis. Ann N Y Acad Sci 2009; 1177: 57-65.
[18] Wang Y, Ji M, Chen L, Wu X, Wang L. Breviscapine reduces acute lung injury induced by left heart ischemic reperfusion in rats by inhibiting the expression of ICAM-1 and IL-18. Exp Ther Med 2013; 6: 1322-1326.
[19] Furuichi K, Wada T, Iwata Y, Kitagawa K, Kobayashi K, Hashimoto H, Ishiwata Y, Asano M, Wang H, Matsushima K, Takeya M, Kuziel WA, Mukaida N, Yokoyama H. CCR2 signaling contributes to ischemia-reperfusion injury in kidney. J Am Soc Nephrol 2003; 14: 2503-2515.
[20] Pan JA, Fan Y, Gandhirajan RK, Madesh M, Zong WX. Hyperactivation of the mammalian degenerin MDEG promotes caspase-8 activation and apoptosis. J Biol Chem 2013; 288: 2952-2963.
[21] Miyajima A, Chen J, Lawrence C, Ledbetter S, Soslow RA, Stern J, Jha S, Pigato J, Lemer ML, Poppas DP, Vaughan ED, Felsen D. Antibody to transforming growth factor-beta ameliorates tubular apoptosis in unilateral ureteral obstruction. Kidney Int 2000; 58: 2301-2313.
[22] Kelly KJ, Dominguez JH. Rapid progression of diabetic nephropathy is linked to inflammation and episodes of acute renal failure. Am J Nephrol 2010; 32: 469-475.
[23] Kelly KJ, Molitoris BA. Acute renal failure in the new millennium: time to consider combination therapy. Semin Nephrol 2000; 20: 4-19.